Available online at www.sciencedirect.com

ScienceDirect

journal homepage: www.intl.elsevierhealth.com/journals/dema

Ultra-high-speed videography of resin–dentin interface failure dynamics under tensile load

Keiichi Hosaka[a,*], *Antonin Tichy*[a,b], *Masaomi Ikeda*[c], *Keiichi Nakagawa*[d], *Alireza Sadr*[e], *Junji Tagami*[a], *Masahiro Takahashi*[a], *Kento Sato*[a], *Yoshihiro Nishitani*[f], *Celso Afonso Klein-Junior*[g], *David H. Pashley*[h], *Masatoshi Nakajima*[a]

[a] *Department of Cariology and Operative Dentistry, Graduate School of Medical and Dental Sciences, Tokyo Medical and Dental University, 1-5-45 Yushima, Bunkyo-ku, Tokyo 113-8510, Japan*

[b] *Institute of Dental Medicine, First Faculty of Medicine of the Charles University and General University Hospital in Prague, Karlovo namesti 32, Prague, 121 11, Czech Republic*

[c] *Department of Oral Prosthetic Engineering, Graduate School of Medical and Dental Sciences, Tokyo Medical and Dental University, 1-5-45 Yushima, Bunkyo-ku, Tokyo 113-8510, Japan*

[d] *Department Bioengineering, Department of Precision Engineering, The University of Tokyo, 7-3-1 Hongo, Bunkyo-ku, Tokyo, 113-8656, Japan*

[e] *Department of Restorative Dentistry, School of Dentistry, University of Washington, 1959 NE Pacific Street, Seattle, Washington, 98195-7456, USA*

[f] *Department of Operative Dentistry, Kagoshima University Graduate School of Medicine, Dentistry and Pharmaceutical Sciences, 2-5-1 Shikata-cho, Kita-ku, Okayama 700-8525, Japan*

[g] *Department of Operative Dentistry, School of Dentistry, Lutheran University of Brazil, Avenue Martinho Lutero, 301. CEP96501-595. Cachoeira do Sul, Rs, Brazil*

[h] *Department of Oral Biology, College of Dental Medicine, Georgia Regents University, 1120 15th Street, CL-2112, Augusta, Georgia, 30912-1129, USA*

ARTICLE INFO

Keywords:
Ultra-high-speed videography
Dental adhesive systems
Micro-tensile bond-strength test
Failure mode
Fractographic analysis
Crack propagation

ABSTRACT

Objectives. Ultra-high-speed (UHS) videography was used to visualize the fracture phenomena at the resin–dentin interface during micro-tensile bond strength (μTBS) test. We also investigated whether UHS videography is applicable for failure-mode analysis.

Methods. Ten human mid-coronal dentin surfaces were bonded using Clearfil SE Bond either in self-etching (SE) or etch-and-rinse (ER) mode. After 24-h water storage, the samples were cut into beams for μTBS test and tested at a cross-head speed of 1 mm/min. The fracture phenomena at the bonded interface were captured using a complementary metal–oxide–semiconductor digital UHS camera at 299,166 frames per second. The failure modes were classified using UHS videography, followed by scanning electron microscopy (SEM) analysis. The failure-mode distributions determined by UHS videography and SEM analysis were statistically analyzed using Fisher's exact test with Bonferroni correction.

Results. The crack-propagation speed exceeded 1,500 km/h. No significant difference was found between the SEM and UHS videography failure-mode distributions in the SE mode.

* *Corresponding author.*
E-mail address: hosaka.ope@tmd.ac.jp (K. Hosaka).

https://doi.org/10.1016/j.dental.2019.04.006

t A significant difference appeared between them in the ER mode. Significant differences in the incidence of cohesive failures within the adhesive and at the adhesive–composite interface between the SE and ER modes were identified by both SEM and UHS videography. *Significance.* UHS videography enabled visualization of the fracture dynamics at the resin–dentin interfaces under tensile load. However, the resolution at such high frame rate was insufficient to classify the failure mode as precisely as that of SEM. Nevertheless, UHS videography can provide more detailed information about the fracture origin and propagation.

1. Introduction

The development of adhesive materials has rapidly advanced over the past decades, and direct composite restorations have become an excellent and long-term reliable treatment option [1–3]. The ability to achieve a reliable and durable bond between the resin and tooth structure is of paramount importance. To evaluate the bonding quality of adhesive materials and study the experimental variables, numerous mechanical bond-strength tests have been developed. Among them, the micro-tensile bond-strength test introduced by Sano et al. [4] has been adopted by many laboratories owing to its in-vitro versatility and reliability [5]. The mechanical tests provide information about the debonding force relative to the bonded area. Even though the correlation between the bond and clinical outcome is weak [6,7], higher bond strength is generally considered to be indicative of effectiveness in the oral environment.

However, the measured bond strength alone does not provide sufficient information about the bond properties [8,9]. The fracture location is also very important, and analysis of the fragments can show differences even among materials with similar bond strengths [10]. The fracture type can be identified after the mechanical test by post-mortem fractographic examination of each failed specimen using light or scanning electron microscopy (SEM) [11]. Conventionally, cohesive and interfacial failures are differentiated based on the characteristic structural properties of the materials. In case more than one layer of the resin–dentin interface is observed at the failed surface, the failure mode is described as mixed. Nevertheless, such observations may not provide accurate information about the weakest point where the fracture has initiated because fracture propagation under stress may not continue in the same layer. In dental ceramics, fractographic methods are available to determine the fracture origin and direction of crack propagation. Among the signs that indicate the crack origin, the presence of a fracture mirror needs to be mentioned, whereas the direction of crack propagation is indicated by the presence of hackles and arrest lines [12–15]. However, these methods cannot be easily applied to dental resin composites because they possess the properties of both brittle materials and polymers [16].

To understand the nature and complexity of interfacial failures, fracture dynamics need to be investigated [17]. To date, only a few attempts have been made to investigate the failure event during bond-strength tests. Previous studies published in 1999 and 2000 used a normal video camera with a frame rate of 25 frames per second (fps) to record the high-speed interfacial-failure events of resin-modified glass ionomer cements [18] and resin-based materials with dentin during a conventional shear bond test [19]. In relation to the previously mentioned studies, we have attempted to use a normal video camera to capture failure events during a micro-tensile bond-strength test (μTBS) in a pilot study. Unfortunately, the frame rate was not sufficiently high to capture the process of the resin–dentin interface failure under μTBS testing because the fracture events occurred at extremely high speed [19].

Over the past decades, notable progress in imaging has been achieved owing to the effort to record fast-moving objects or events that are too fast or complex for a human eye to follow in real time. In 1948, “high-speed photography” was arbitrarily defined by the Society of Motion Picture and Television Engineers as any motion-picture photography beyond 250 fps with exposure times of 1 ms or less. The Focal Encyclopedia of Photography [20] distinguishes four categories of high-speed imaging: (1) “high speed” with a frame rate of 50–500 fps, (2) “very high speed” of 500–10,000 fps, (3) “ultra high speed” (UHS) of 10,000–10,000,000 fps, and (4) “super high speed” of more than 10 million fps. New video systems equipped with complementary metal–oxide–semiconductor (CMOS) chips used in scientific research, military field, and industry are able to reach frame rate of up to 1 million fps [21], which corresponds to the UHS category.

In addition to the frame rate and shutter speed, photograph resolution is of major importance. Generally, video cameras enable increase in the frame rate by decreasing the frame resolution. Therefore, using a maximal frame rate may not be ideal in cases where good resolution is necessary. In addition, quality pictures can only be obtained using proper lighting. Light sources can be divided in two categories: continuous and pulsed synchronized with the shutter [21]. Metal halide lamps are commonly used in the field of engineering; however, they generate considerable heat and can damage the dental-tissue specimens. To prevent any heat influence, the use of a pulsed diode laser-light source synchronized with the shutter is preferred.

The purpose of the present study is to visually investigate the fracture phenomena at the resin–dentin interface during a micro-tensile bond-strength test. By using a UHS video camera with a frame rate of almost 300,000 fps, the fracture events that occurred during the test were recorded and subsequently ana-

Table 1 – Compositions of the materials used in this study.

Material	Composition (Batch number)	Application procedure
Clearfil SE Bond (CSB; Kuraray Noritake Dental, Tokyo Japan)	Primer: 10-MDP, HEMA, hydrophilic dimethacrylate, camphorquinone, N,N-diethanol p-toludine, water (01162 A)	[SE mode]
	Adhesive: 10-MDP, Bis-GMA, HEMA, hydrophilic dimethacrylate, camphorquinone, N,N-diethanol p-toludine, silanized colloidal silica. (01746 A)	Apply primer for 20 s, strong air dry
		Apply adhesive and gently air dry Light-cure for 10 s. [ER mode] Etch for 15 s and rinse with water Apply ethanol to keep the surfaces wet 50% ethanol/50% adhesive double application Air blow for 3 s Apply adhesive neatly Light-cure for 10 s
K-etchant (Kuraray Noritake Dental, Tokyo Japan)	40% phosphoric acid, thickener	[ER mode] Etch for 15 s and rinse with water
Clearfil AP-X (Kuraray Noritake Dental, Tokyo Japan)	Bis-GMA, TEGDMA, camphorquinone, photo initiators, pigments, silanated barium glass, silanated silica (01124A)	Apply a layer <2 mm to the bonded surface Light-cure for 40 s Repeat three times to achieve a height of 5 mm

Abbreviations. 10-MDP: 10-methacryloyloxydecyl dihydrogen phosphate, Bis-GMA: bisphenol-glycidyl methacrylate: HEMA, hydroxyethyl methacrylate.

lyzed frame by frame to identify the crack origin and observe its propagation. The null hypothesis of the test was that no difference could occur in the failure mode determined by UHS videography and SEM.

2. Materials and methods

2.1. *Teeth*

Ten caries-free human third molars were collected after obtaining informed consent from the subjects under Protocol No. 2014-022, which was reviewed and approved by the Ethics Committee of Tokyo Medical and Dental University, and were stored frozen before use within one month of extraction. The occlusal dental tissues were removed using a low-speed diamond saw (Isomet, Buehler, Illinois, US), and the mid-coronal flat dentin surfaces of the human molars were ground using a 600-grit SiC paper to create a standardized smear layer. The specimens were randomly allocated to two groups for adhesive application.

2.2. *Adhesive application and composite build-up*

A two-step self-etch adhesive (Clearfil SE Bond, Kuraray Noritake Dental Corp., Tokyo, Japan, Table 1) was applied to the prepared dentin surfaces. Half of the teeth were treated in a self-etch (SE) mode, and the other half were treated in an etch-and-rinse (ER) mode using an ethanol wet-bonding technique [28]. In the SE mode, the primer was applied using an applicator brush, left in place for 20 s, and dried using mild air for more than 5 s. In the ER mode, the specimens were acid-etched using a 40% phosphoric-acid gel (K-etchant gel, Kuraray Noritake Dental Corp., Table 1) for 15 s, rinsed with water, and inverted on wet lint-free tissues until bonded. The primer was created by mixing 50 mass% adhesive of Clearfil SE Bond with 50 mass% ethanol. This primer was applied to the ethanol-saturated acid-etched dentin in two layers. A generous amount of primer was employed as the first layer and gently agitated using a micro brush for 10 s. A second application was made and agitated for 10 s. The ethanol solvent was evaporated from the primed surface using a gentle stream of air. In both modes, the bonding agent was applied to the primed dentin using an applicator brush, a uniform layer was created using gentle air flow, and the bonding agent was light-cured for 10 s using a LED light-curing unit (Pencure 2000, Morita Corp., Tokyo, Japan) with a light output of >600 $mW \cdot cm^{-2}$. After light-curing of the adhesive, a resin composite (Shade-A2, Clearfil AP-X, Kuraray Noritake Dental Corp., Table 1) was used for incremental build-up to a height of 5.0 mm to ensure a sufficient bulk for the μTBS test. Each increment had a thickness of up to 2.0 mm and was light-cured for 40 s using the same light-curing unit.

2.3. *Micro-tensile bond strength testing and failure-mode analysis*

After the bonded teeth had been stored in distilled water for 24 h at 37 °C, they were longitudinally sectioned into beams (surface area: 1.4 mm × 0.7 mm) using a low-speed diamond saw (Isomet, Buehler, Illinois, US) under water-spray coolant. Ten beams, located at the center of each tooth, were assigned to each group (n = 50). The beams were individually bonded to a tensile testing jig of a universal testing machine (EZ Test, Shi-

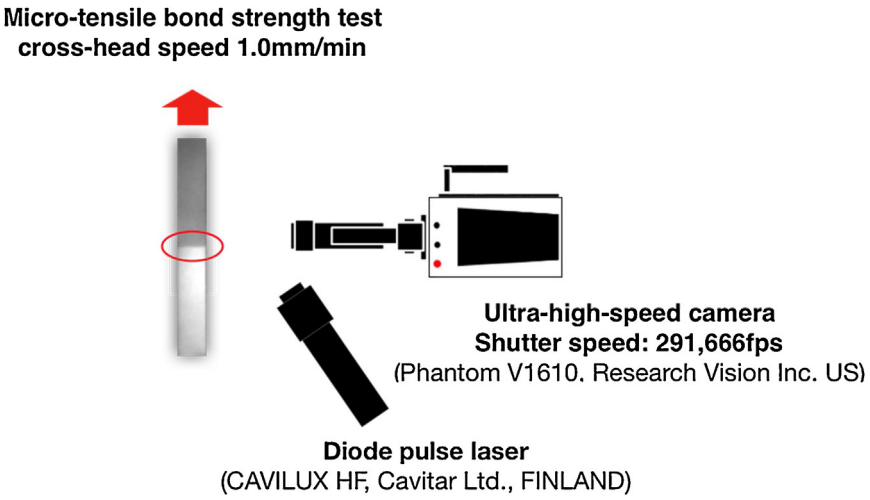

Fig. 1 – Scheme of ultra-high-speed imaging technique during micro-tensile bond strength test.

madzu Co., Kyoto, Japan) using cyanoacrylate adhesive (Zapit, Dental Ventures of America, Corona, CA) and loaded with tension at a cross-head speed of 1 mm/min until failure. The load in newton at failure was divided by the cross-sectional area to calculate μTBS (MPa).

The fractured specimens were mounted on brass stubs, sputter-coated with gold, and observed using SEM (JSM-5310, JEOL, Tokyo, Japan) at standardized magnifications to evaluate the failure mode. The failure modes were classified as follows: (1) cohesive failure in the dentin, (2) dentin–adhesive interfacial failure, (3) cohesive failure in the adhesive resin, (4) adhesive–composite interfacial failure, (5) cohesive failure in the composite resin, (6) mixed failure of (1) and (2), (7) mixed failure of (2) and (3), and (8) mixed failure of (3) and (4). The failure-mode distributions of all fractured specimens were calculated and expressed in percentages.

2.4. *UHS imaging technique*

The failure images of the bonded interface in each specimen were captured using a CMOS digital UHS camera (Phantom V1610, Vision Research Inc., New Jersey, US), which was equipped with a Leica, 9.2× magnification lens (Fig. 1) and an image resolution of 256 by 112 pixels, at a maximum rate of 291,666 fps. A pulsed diode-laser light source (pulse width: 60 ns, CAVILUX HF for High-Speed Illumination, CAVITAR, Finland) was synchronized with the shutter speed of the UHS camera. The captured images were dynamically analyzed using camera-control software (Camera Control Software, PCC, Vision Research Inc.) to identify the crack initiation, propagation, and opening. The crack-location patterns were analyzed as far as possible according to the appearance of the failure by replaying the fracture-image sequences and were classified into the same eight categories described earlier for SEM analysis.

2.5. *Statistical analysis*

The Fisher's exact test with Bonferroni correction at significance level $\alpha = 0.05$ was performed to statistically analyze the failure-mode distributions determined using SEM and UHS videography in both adhesive application modes. The two application modes were subjected to the same test ($\alpha = 0.05$) to determine whether a significant difference occurred between their failure-mode distributions. The μTBS values in the SE mode were not normally distributed according to the Shapiro–Wilk test ($p < 0.05$). Therefore, the μTBS data were analyzed using the Wilcoxon rank-sum test at 5% significant level to test the effect of the application modes on μTBS.

3. Results

The extremely rapid fracture phenomena at the resin–dentin interface were successfully visualized using the UHS camera. The crack initiation, propagation, and opening, as well as the detached fragments with various sizes, were observed and are shown in Figs. 4–6 and Multimedia Components 1–5. Despite the immense frame rate of almost 300,000 fps, only one frame in each video captured the propagating crack. The speed of the fracture propagation therefore surpassed 1,500 km/h at a specimen thickness of 1.4 mm, and the frame interval was 3.428 μs.

The summary of the failure-mode distributions (in percentages) for both the adhesive application modes and detection methods is listed in Table 2. In the SE mode, the Fisher's exact test with a Bonferroni correction revealed no significant difference between the SEM analysis and UHS videography. In both analysis methods, the specimens predominantly failed cohesively in the adhesive resin, at the interface between the adhesive and resin composite, or in their combination. In contrast, no failure was observed at the dentin–adhesive interface and within the resin composite. In the ER mode, statistically significant differences were observed between the two failure-mode distributions in the dentin–adhesive interfacial failures ($p = 0.001$), and cohesive failures were observed in the adhesive resin ($p = 0.001$). The SEM analysis identified that 48% of the specimens fractured cohesively in the adhesive, whereas the rest was mainly distributed between the dentin–adhesive interfacial, dentinal cohesive, and their

Table 2 – Failure mode distribution [%] of both observation methods.

Application mode	Observation method	Failure mode pattern [%]							
		(1) Cohesive in dentin	(2) Dentin–adhesive interfacial failure	(3) Cohesive in adhesive resin	(4) Adhesive–composite interfacial failure	(5) Cohesive in composite resin	(6) Mix of (1) + (2)	(7) Mix of (2) + (3)	(8) Mix of (3) + (4)
SE mode	SEM	10	0	30^{A}	30^{B}	0	0	0	30
	UHS	12	0	28^{a}	32^{b}	0	0	0	28
ER mode	SEM	8	16^{*}	$48^{A\#}$	4^{B}	0	20	4	0
	UHS	0	48^{*}	$24^{a\#}$	4^{b}	0	24	0	0

Abbreviations: SEM: Scanning electron microscopy. UHS: Ultra high-speed imaging. The same superscript letters and the same marks indicate significant differences ($p < 0.05$).

Table 3 – Micro-tensile bond strength values (n = 50): Mean (S. D.).

Application mode	SE mode		ER mode
μTBS (MPa)	65.8 (10.2)	$P < 0.05$	71.7 (10.4)

Abbreviations: SE: self-etch, ER: etch-and-rinse.

mixed fractures. According to the UHS videography, 48% of the failures occurred at the dentin–adhesive interface, followed by cohesive failures within the adhesive (24%) and mixed failures within the dentin and at the dentin–adhesive interface (24%). Interestingly, no pure dentinal cohesive fracture was identified in the ER mode by the UHS videography compared with four pure dentinal cohesive fractures (8%) observed by SEM. In the SE mode, no cohesive fracture within the resin composite was identified. The statistical analysis also indicated that the SEM and UHS analyses revealed significant differences between the failure-mode distributions of the SE and ER modes. Between both application modes (SE versus ER modes), significant differences were found in the cohesive failures within the adhesive layer (SEM: $p = 0.001$, UHS: $p = 0.021$) and the adhesive–composite interfacial failures (SEM: $p = 0.001$, UHS: $p = 0.015$).

Table 3 lists the mean μTBS values of the Clearfil SE Bond to the dentin in the two application modes. A significant difference in μTBS was found between the SE and ER modes ($p = 0.012$).

4. Discussion

μTBS test is the most common method to evaluate the bonding effectiveness to enamel and dentin in the dental academia and industry [22]. Combined with the fractographic analysis using SEM, which can identify each material on the fractured surfaces, this procedure is considered standard for bonding evaluation. However, the SEM analysis cannot provide sufficient information on the dynamic phenomena of fracture at the resin–dentin interface, e.g., crack initiation and propagation. An adhesive failure can propagate into the dental substrate or the resin composite, or conversely, an originally cohesive fracture within the dentin or resin composite may spread to the adhesive layer. In spite of the increased popularity gained by the μTBS test, the fracture dynamics have never been investigated in real time.

In the dental research field, Griffiths et al. used a video camera with a frame rate of 25 fps to capture the fracture during a conventional shear bond-strength test and successfully visualized it [19]. However, our pilot study showed that such frame rate is not sufficient to capture the images of a propagating failure under the μTBS test. Therefore, UHS videography was used and presented as a novel option to observe the fracture phenomena during a μTBS test in real time. In the pilot study using a UHS camera, various frame rates ranging from 1,000 to 1,000,000 fps were tested. Because the resolution rapidly decreased with increasing frame rate, the highest achievable frame rates did not provide sufficient image quality for crack observation, and hence, the frame rate of 299,166 fps was chosen as the most appropriate. Even though its resolution of 256×112 pixels was not perfect, lower frame rates were

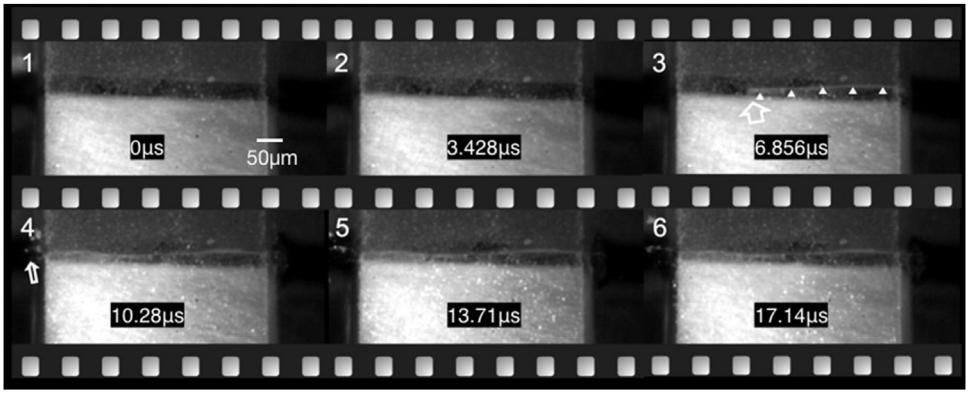

Fig. 2 – Ultra-high-speed photographic visualization of the crack propagation in the resin–dentin interface created by Clearfil SE Bond in the SE mode under a micro-tensile load (Multimedia Component 1 in Appendix A).
Selection of frames captured by the ultra-high-speed camera showing the crack propagation within the adhesive layer of Clearfil SE Bond in the SE mode. The front of the crack propagation is indicated (white arrow in frame 3). Flying fragments from the crack were observed (white arrow in frame 4). Frame rate: 291,666 fps (frame interval 3.428 μs); resolution: 256 × 112.

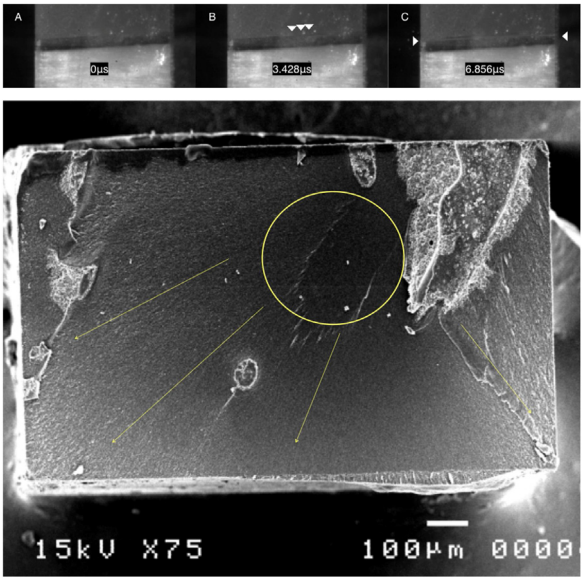

Fig. 3 – Crack opening at the adhesive–composite interface in the specimen created by Clearfil SE Bond in the SE mode (Appnedix A in Appnedix A).
(Top) Sequential images captured by the ultra-high-speed camera under a tensile load. (A) Before crack initiation. (B) Crack initiated at the center of the adhesive–composite interface. (C) The crack propagated toward the edges. Frame rate: 291,666 fps (frame interval 3.428 μs); resolution: 256 × 112.
(Bottom) SEM image of the debonded surface at the dentin side of the same specimen shown above. The yellow circle indicates the corresponding failure origin, and the yellow arrows indicate the "presumed" crack-propagation path.

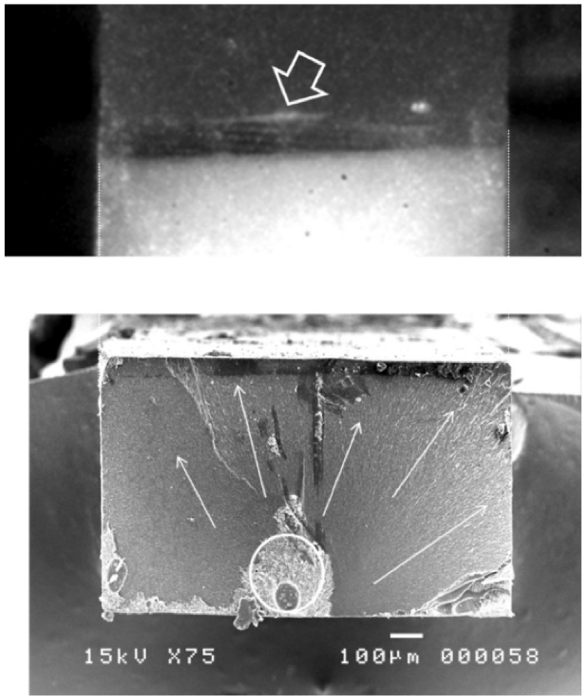

Fig. 4 – Representative the ultra-high-speed image of the crack initiation at the interface between the adhesive layer and composite in the SE mode of Clearfil SE Bond (Appnedix A in Appendix A).
(Top) The white arrow indicates the crack initiation at the middle of the adhesive–composite interface. Frame rate: 291,666 fps (frame interval 3.428 μs); resolution: 256 × 112.
(Bottom) SEM image of the debonded surface at the dentin side of the same specimen shown above. The circle indicates the corresponding location of the crack initiation. The white arrows indicate the direction of crack propagation.

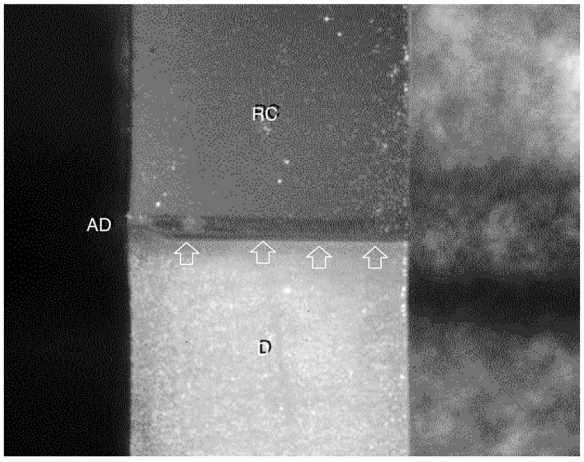

Fig. 5 – Representative the ultra-high-speed image of the crack opening at the interface between the dentin and adhesive layer in the ER mode of Clearfil SE Bond (Appnedix A in Appendix A).
The arrows indicate the crack opening. Abbreviations: RC: resin composite, AD: adhesive layer, D: dentin. Frame rate: 25,000 fps (frame interval 40 μs); resolution: 768 × 768.

unable to reliably catch the propagation of the fracture. On the basis of this information, we calculated that the speed of the crack propagation in the resin–dentin bonded specimens created in this study exceeded 1,500 km/h. To increase the chance of capturing the crack propagation, the dimensions of the specimens were set to 1.4 mm × 0.7 mm (approximately corresponding to 1-mm^2 area), and their longer side was recorded by the camera. By using these settings, the cracks were clearly captured and visualized Multimedia Components 1–5 and Figs. 2–6). More specifically, the crack initiation could be seen in Multimedia Components 2 and 3 and Figs. 3 and 4, and the crack propagation was recorded in Multimedia Components 1–3 and Figs. 2–4.

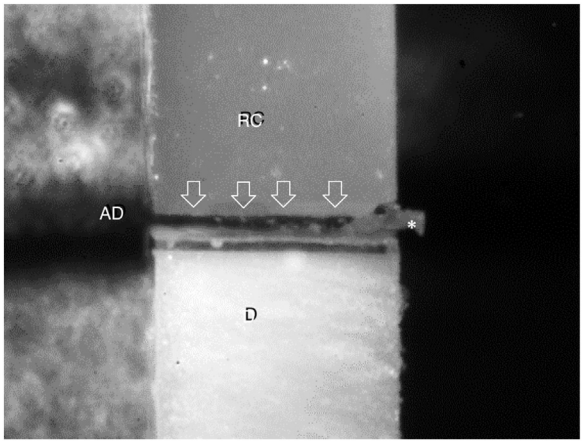

Fig. 6 – Representative the ultra-high-speed image of the crack opening at the interface between the adhesive layer and composite in the SE mode of Clearfil SE Bond (Appnedix A in Appendix A).
The arrows indicate the crack opening. The asterisk shows the bulk fragment of the composite. Abbreviations: RC: resin composite, AD: adhesive layer, D: dentin. Frame rate: 10,000 fps (frame interval 100 μs); resolution: 608 × 608

The comparison of the UHS videography and SEM fractographic analysis in the SE mode showed very similar failure-mode distributions, and no statistically significant difference was found between them. Nevertheless, in contradiction to the null hypothesis, these methods demonstrated different results in the ER mode. The UHS videography identified that almost half of the failures occurred at the dentin–adhesive interface. In comparison, the SEM analysis also exhibited more mixed failures in the dentin and dentin–adhesive interface, few adhesive cohesive fractures, and no dentinal cohesive fractures. The resolution of the UHS camera at this frame rate appeared to be insufficient to properly differentiate the layers at the basal side of the adhesive interface. The incorrect identification of the cohesive fractures in the dentin was probably caused by the fact that they occurred closer to the dentin–adhesive interface compared with those in the SE mode, which could be attributed to the existence of a relatively deeply phosphoric-acid etched dentin in the ER mode compared with the mildly acidic SE mode. We speculate that the demineralization caused by phosphoric-acid etching may have decreased the cohesive strength of the dentin surface, resulting in its fracture immediately below the interface [23]. The higher quantity of mixed dentinal cohesive and dentin-adhesive interfacial fractures in the ER mode appeared to corroborate this hypothesis as the crack could cross the border between these two fine layers.

To evaluate the differences between the ER and SE approaches, the experimental design should avoid all other influences. The bond strength between the adhesives and tooth structures is known to be influenced by a large number of variables such as the composite type, bonding area, cross-head speed, substrate, specimen storage conditions, and thermocycling [24]. Furthermore, the thickness [25,26] and degree of conversion [27] of the adhesive layer also affect μTBS. Therefore, in the present study, only one adhesive (Clearfil SE Bond) in its two recommended application modes was used to eliminate the other variables. Thus, the results of the μTBS test and subsequent failure-mode analysis should only reflect the differences in the etching depth and thickness of the hybrid layer produced by the two application modes.

Both SEM and UHS failure-mode analysis revealed significant differences between the failure mode distributions of the SE and ER modes. In the ER mode, cohesive failures within the adhesive layer were significantly more frequent (48%) than those in the SE mode (30%), which demonstrated more fractures at the interface between the adhesive and resin composite, whereas the ER mode significantly failed more often at the dentin–adhesive interface (UHS: $p = 0.015$; and SEM $p < 0.001$). A significant difference was also found between the μTBS values of the two application modes of the Clearfil SE Bond. These results show that the adhesive-application mode exerts an indisputable effect on the bonding performance and failure mechanism. However, generalizing these results is impossible because their long-term bonding efficiency needs to be evaluated as well, and more adhesive systems should be tested using these two application modes.

Despite the fact that the UHS videography was not as accurate as SEM in the failure-mode analysis, it enabled

visualization of the failure dynamics during the μTBS test for the first time. Because the high-speed imaging field is quickly evolving, the shortcomings of the UHS videography mentioned in this study is highly probable that will soon be overcome, and cameras with higher resolutions will be developed. The identification of the initial point of the crack and its propagation provides complementary information to the static SEM observation, which only shows the layer with the lowest resistance to crack propagation. Information from UHS videography can provide more clarity to the fracture dynamics in the future and can hopefully help correlate in-vitro experiments to in-vivo failures. Future studies should include more variables in terms of specimen preparation, storage conditions, and restorative materials. Moreover, for correlation to in-vivo failures, fracture dynamics should also be observed during mechanical tests other than micro-tensile load, such as shear, compression, flexion, cyclic fatigue, and similar conditions.

5. Conclusion

The null hypothesis tested in this study was partially rejected because a difference was found between the failure-mode distributions determined by the UHS videography and SEM analysis in the ER mode. This difference could be attributed to insufficient resolution of the camera when a very high frame rate of 299,166 fps was used. However, the UHS videography enabled recording of the fracture phenomena during the μTBS test for the first time. We also estimated that the crack propagated at a speed exceeding 1,500 km/h as it was always captured in only one frame despite their 3.428-μs interval. In the future, UHS videography with even higher frame rate and resolution can help in understanding the mechanism of fracture dynamics at the resin–dentin interface and therefore aid in further development of adhesive systems.

Acknowledgement/Funding

This work was supported by the Ministry of Education, Culture, Sports, Science and Technology of Japan (Grant Numbers, 26462873, 15K11108, 17K17125, and 18K09571).

Appendix A. Supplementary data

Supplementary material related to this article can be found, in the online version, at doi:https://doi.org/10.1016/j.dental.2019.04.006.

REFERENCES

[1] Peumans M, De Munck J, Mine A, Van Meerbeek B. Clinical effectiveness of contemporary adhesives for the restoration of non-carious cervical lesions. A systematic review. Dent Mater 2014;30:1089–103.
[2] Heintze SD, Rousson V, Hickel R. Clinical effectiveness of direct anterior restorations—a meta-analysis. Dent Mater 2015;31:481–95.
[3] Heintze SD, Rousson V. Clinical effectiveness of direct class II restorations—a meta-analysis. J Adhes Dent 2012;14:407–31.
[4] Sano H, Ciucchi B, Matthews WG, Pashley DH. Tensile properties of mineralized and demineralized human and bovine dentin. J Dent Res 1994;73:1205–11.
[5] Scherrer SS, Cesar PF, Swain MV. Direct comparison of the bond strength results of the different test methods: a critical literature review. Dent Mater 2010;26:e78–93.
[6] Van Meerbeek B, Peumans M, Poitevin A, Mine A, Van Ende A, Neves A, et al. Relationship between bond-strength tests and clinical outcomes. Dent Mater 2010;26:e100–21.
[7] Heintze SD, Thunpithayakul C, Armstrong SR, Rousson V. Correlation between microtensile bond strength data and clinical outcome of class V restorations. Dent Mater 2011;27:114–25.
[8] Sirisha K, Rambabu T, Ravishankar Y, Ravikumar P. Validity of bond strength tests: a critical review-part II. J Conserv Dent 2014;17:420–6.
[9] Tam LE, Pilliar RM. Fracture surface characterization of dentin-bonded interfacial fracture toughness specimens. J Dent Res 1994;73:607–19.
[10] Armstrong SR, Boyer DB, Keller JC. Microtensile bond strength testing and failure analysis of two dentin adhesives. Dent Mater 1998;14:44–50.
[11] Armstrong S, Geraldeli S, Maia R, Raposo LH, Soares CJ, Yamagawa J. Adhesion to tooth structure: a critical review of "micro" bond strength test methods. Dent Mater 2010;26:e50–62.
[12] Quinn GD. NIST recommended practice guide fractography of ceramics and glasses. 2nd ed Special publication (NIST SP); 2016.
[13] Scherrer SS, Quinn GD, Quinn JB. Fractographic failure analysis of a Procera AllCeram crown using stereo and scanning electron microscopy. Dent Mater 2008;24:1107–13.
[14] Scherrer SS, Quinn JB, Quinn GD, Kelly JR. Failure analysis of ceramic clinical cases using qualitative fractography. Int J Prosthodont 2006;19:185–92.
[15] Quinn JB, Quinn GD, Kelly JR, Scherrer SS. Fractographic analyses of three ceramic whole crown restoration failures. Dent Mater 2005;21:920–9.
[16] Quinn JB, Scherrer SS, Quinn GD. The increasing role of fractography in the dental community. In: Varner JR, Quinn GD, Wightman M, editors. Fractography of glasses and ceramics V. New Jersey: Wiley InterScience; 2007. p. 253–70.
[17] Marshall SJ, Bayne SC, Baier R, Tomsia AP, Marshall GW. A review of adhesion science. Dent Mater 2010;26:e11–6.
[18] Sidhu SK, Sherriff M, Watson TF. Failure of resin-modified glass-ionomers subjected to shear loading. J Dent 1999;27:373–81.
[19] Griffiths BM, Watson TF, Pagliari DE, Pilecki P, Sherriff M. Video rate confocal microscopic imaging of dentin/adhesive interfacial failure under load. Am J Dent 2000;13:271–9.
[20] Fuller PWW. High-speed cinematography. In: Peres MR, editor. Focal Encyclopedia of Photography. 4th ed. Woburn, MA: Focal Press; 2007. p. 539.
[21] Fuller PWW. An introduction to high-speed photography and photonics. Imaging Sci J 2009;57:293–302.
[22] Ferracane JL, Hilton TJ, Sakaguchi RL. Introduction to and outcomes of the conference on adhesion in dentistry. Dent Mater 2010;26:105–7.
[23] Kato G, Nakabayashi N. Effect of phosphoric acid concentration on wet-bonding to etched dentin. Dent Mater 1996;12:250–5.
[24] Leloup G, D'Hoore W, Bouter D, Degrange M, Vreven J. Meta-analytical review of factors involved in dentin adherence. J Dent Res 2001;80:1605–14.
[25] de Menezes FC, da Silva SB, Valentino TA, Oliveira MA, Rastelli AN, Concalves Lde S. Evaluation of bond strength

and thickness of adhesive layer according to the techniques of applying adhesives in composite resin restorations. Quintessence Int 2013;44:9–15.

[26] AdA Neves, Coutinho E, Poitevin A, Van der Sloten J, Van Meerbeek B, Van Oosterwyck H. Influence of joint component mechanical properties and adhesive layer thickness on stress distribution in micro-tensile bond strength specimens. Dent Mater 2009;25:4–12.

[27] Sato K, Hosaka K, Takahashi M, Ikeda M, Tian F, Komada W, et al. Dentin bonding durability of two-step self-etch adhesives with improved degree of conversion of adhesive resins. J Adhes Dent 2017;19:31–7.

[28] Hosaka K, Nishitani Y, Tagami J, Yoshiyama M, Brackett WW, Agee KA, Tay FR, Pashley DHJ. Durability of resin-dentin bonds to water- vs. ethanol-saturated dentin. Dent Res 2009;88(2):146–51, http://dx.doi.org/10.1177/0022034508328910. PMID: 19278986.